Chemosphere 82 (2011) 751–758

Contents lists available at ScienceDirect

Chemosphere

journal homepage: www.elsevier.com/locate/chemosphere

Removal of 4,4′-dichlorinated biphenyl from aqueous solution using methyl methacrylate grafted multiwalled carbon nanotubes

Dadong Shao, Jun Hu, Zhongqing Jiang, Xiangke Wang *

Key Laboratory of Novel Thin Film Solar Cells, Institute of Plasma Physics, Chinese Academy of Sciences, P.O. Box 1126, Hefei 230031, PR China

ARTICLE INFO

Article history:
Received 16 April 2010
Received in revised form 22 October 2010
Accepted 31 October 2010
Available online 24 November 2010

Keywords:
4,4′-DCB
MWCNTs
Adsorption
Methyl methacrylate
Plasma technique
Water remediation

ABSTRACT

Methyl methacrylate (MMA) is grafted on multiwalled carbon nanotubes (MWCNTs) by using N_2 plasma technique. The MMA grafted MWCNTs (MWCNT-*g*-pMMA) are characterized by using Raman spectroscopy, powder X-ray diffraction, X-ray photoelectron spectroscopy, thermo gravimetric analysis–differential thermal analysis (TGA–DTA), and potentiometric acid-base titration method. The application of MWCNT-*g*-pMMA in the removal of 4,4′-dichlorinated biphenyl (4,4′-DCB) from large volumes of aqueous solutions is investigated under ambient conditions. The results indicate that the adsorption of 4,4′-DCB on MWCNT-*g*-pMMA is much higher than that of 4,4′-DCB on MWCNTs, and the adsorbed 4,4′-DCB is difficult to be thermally decomposed from MWCNT-*g*-pMMA according to the TGA–DTA analysis. MWCNT-*g*-pMMA are suitable materials in the preconcentration and immobilization of polychlorinated biphenyls (PCBs) from large volumes of aqueous solutions in environmental pollution cleanup.

1. Introduction

Polychlorinated biphenyls (PCBs), classic persistent organic pollutants, are highly toxic and resistant to degradation (Gjessing et al., 2007; Yang et al., 2007). Although they are not allowed to produce now, PCBs had ever been used in large amount and now they are ubiquitous persistent contaminants in the natural environment (Skoglund et al., 1996; Werner et al., 2006), and can be easily bio-accumulated in food chains (Sober et al., 2006). The remediation of PCB pollution in the environment has become a major worldwide problem. The knowledge of PCB adsorption on different adsorbents is important for the understanding and remediation of PCB pollution. Various technologies have been used for the treatment of PCB pollution. Adsorption is one of the most cost-effective technologies for the removal of organic pollutants. Therefore, the novel adsorbents with high adsorption capacity are crucial for the elimination of PCBs in the environmental pollution cleanup. Low chlorinated PCBs are significant for the evaluation of the transport and overall fate of PCBs because of their relatively high aqueous solubility (Adeel et al., 1997). Dichlorobiphenyls and trichlorobiphenyls are the primary PCBs in the environment (Adeel et al., 1997). Thereby, 4,4-dichlorobiphenyls (4,4′-DCB) is selected as the model of PCBs in this study.

Carbon nanotubes (CNTs) have attracted increased interest in multidisciplinary area and have come into the view as a kind of fascinating materials since their discovery by Iijima (1991). CNTs are relatively new adsorbents and have been proven to possess excellent adsorption ability to remove many kinds of organic pollutants from wastewater (Long and Yang, 2001; Gotovac et al., 2006). Moreover, many studies showed that CNTs were effective adsorbents for organic pollutants in solid phase extraction and water pollution cleanup compared to common carbon materials, such as activated carbon (Wang et al., 2007) and C18 (Liu et al., 2004; Pyrzynska et al., 2007), which suggested that CNTs were efficient materials in the removal of organic pollutants from large volumes of aqueous solutions. However, less surface functional groups, poor chemical and biological compatibility, and inherent insolubility in most organic and inorganic solutions greatly restrict the application of CNTs in real work (Qin et al., 2004; Hong et al., 2006). Thereby, recent researches on CNTs have been extended to the surface modification of CNTs with some special functional groups to improve the compatibility and dispersion property of CNTs. Most modification methods are mainly focused on conventional chemical techniques. However, the conventional chemical modification methods can cause environmental pollution because large amounts of chemicals are used and some toxic chemical pollutants are generated in the modification processes. Although the chemical modification can graft functional groups on the surfaces of CNTs effectively, the shortcoming of large amounts of toxic chemicals used and generated in the modification processes is itself harmful to the environment and human health. Plasma induced grafting treatment is an environmental friendly and effective method to modify

* Corresponding author. Tel.: +86 551 5592788; fax: +86 551 5591310.
E-mail address: xkwang@ipp.ac.cn (X. Wang).

0045-6535/$ - see front matter © 2010 Elsevier Ltd. All rights reserved.
doi:10.1016/j.chemosphere.2010.10.086

material surface properties, such as grafting functional groups on CNT surfaces and alter the surface morphologies of CNTs (Lewis et al., 2007; Shao et al., 2009). Moreover, plasma induced grafting processes can introduce functional groups to material surfaces without altering the material bulk properties (Chevallier et al., 2001; Olander et al., 2002), and the monomer is not necessarily preserved in the plasma grafting processes (Zhang et al., 2004). Plasma technique is a very promising method to modify the surface properties and to graft functional groups on CNT surfaces, which is crucial for the application of CNTs in the removal of many kinds of organic and inorganic pollutants from large volumes of aqueous solutions in environmental pollution cleanup.

Polymeric materials can remove organic pollutants effectively by forming strong complexes with organic pollutants. PCBs and polymers are lipophilic materials, the interaction of PCBs and polymers in aqueous solution can reduce the concentration of PCBs in water (Pascall et al., 2005). Endo et al. (2005) studied the concentration of PCBs in beached resin pellets. Yoon et al. (2003) reported that endocrine disruptors (including PCBs, dichlorodiphenyltrichloroethane, and hexachlorocyclohexane) were removed efficiently by using hydrophobic polydimethylsiloxane membranes without any decomposition or denaturation of milk components. Pascall et al. (2005) reported that PCBs were effectively removed from aqueous solutions by using polyethylene, polyvinyl chloride, and polystyrene films. Polm(methyl methacrylate) (pMMA), one of the most widely used polymers, itself and its based materials can adsorb organic compounds (such as chlorinated contaminants (Yampolskii and Bondarenko, 1998; Das et al., 2006), toluene (Dubreuil et al., 2003), phenol (Li et al., 2004), and cyclohexane/cyclohexene (Shen et al., 2007)) from large volumes of aqueous solutions effectively by forming strong complexes. However, the pMMA in aqueous solution can form sedimentation easily, which reduces the adsorption ability of pMMA in the removal of organic pollutants from aqueous solutions. If pMMA molecules are grafted on the surfaces of CNTs, the sedimentation of pMMA is avoided and the surface functional groups of CNTs are also enhanced. The grafting of pMMA on CNTs can be achieved by chemical method (Koshio et al., 2001; Baskaran et al., 2004; Hwang et al., 2004; Kong et al., 2004). However, to our best knowledge, no literature is available about the grafting pMMA on CNTs using plasma technique, and its application in organic pollutant cleanup. Herein, we synthesized the methyl methacrylate (MMA) grafted multiwalled carbon nanotubes (MWCNTs) (denoted as MWCNT-*g*-pMMA) by using N_2 plasma induced grafting technique. The synthesized MWCNT-*g*-pMMA were characterized by using Raman spectroscopy, powder X-ray diffraction (XRD), X-ray photoelectron spectroscopy (XPS), thermo gravimetric analysis–differential thermal analysis (TGA–DTA), scanning electron microscopy (SEM), and potentiometric acid–base titration. The prepared MWCNT-*g*-pMMA were applied to remove 4,4′-DCB from large volumes of aqueous solutions.

2. Experimental

2.1. Chemical materials

All chemicals used in the experiments were purchased in analytical grade. 4,4′-DCB (>99% purity) was purchased from Accu Standard Inc. (New Haven, USA). MWCNTs were prepared by using chemical vapor deposition of acetylene in a hydrogen flow at 760 °C using Ni–Fe nanoparticles as catalysts (Shao et al., 2009). MWCNTs were added into 3 M HNO_3 solution and ultrasonically stirred for 24 h to remove the hemispherical caps of the nanotubes, and then filtrated and rinsed with Milli-Q water until the pH of the suspension reached about 6, and calcined at 450 °C for 24 h to remove the amorphous carbon after drying at 80 °C.

2.2. Plasma induced grafting procedure

Firstly, 3.0 g MWCNTs were treated by using N_2 plasma for 40 min at a pressure of 10 Pa, a power of 70 W, a voltage of 650 V, and a current of 60 mA in a custom-built grafting reactor under continuous stirring. Then plasma treated MWCNTs were heated to 80 °C and 50 mL MMA solution was injected into the grafting reactor. MMA was grafted on the plasma treated MWCNTs at 80 °C for 24 h under continuous stirring. The derived samples were washed with acetone thoroughly to remove the surface adsorbed MMA. Finally, the samples were dried in an oven at 95 °C for 24 h, and MWCNT-*g*-pMMA materials were obtained and used in the experiments.

2.3. Characterization

MWCNTs and MWCNT-*g*-pMMA were characterized by Raman spectroscopy, XRD, XPS, SEM, and TGA–DTA. Raman spectroscopy was carried out on a LabRam HR Raman spectrometer excited at 514.5 nm by Ar^+ laser. The structures of MWCNTs and MWCNT-*g*-pMMA were analyzed by XRD on a RigaKu D/max 2550 X-ray Diffractometer using Cu Kα radiation ($\lambda = 0.1541$ nm) in the step of $0.05^\circ\ min^{-1}$ from 5 to 70° (2θ) at room temperature. XPS measurements were performed with an ESCALab220i-XL electron spectrometer from VG Scientific using 300 W Al Kα radiations at a chamber pressure of 3×10^{-9} mbar. SEM measurements were carried out by using a JSM-6320F FE-SEM (JEOL). The potentiometric acid–base titrations of the samples were performed at 20 ± 1 °C with a Mettler Toledo DL50 titration apparatus under Ar gas condition, using $NaClO_4$ as background electrolyte and NaOH as titration solution.

The MWCNTs and MWCNT-*g*-pMMA were characterized by using N_2 adsorption–desorption isotherms. N_2-BET measurements were performed by using a Micromeritics ASAP 2020 accelerated surface area and porosimetry analyzer. The specific surface areas were determined from Brunauer–Emmett–Teller equation, the average pore diameters and pore specific volumes were determined from Barret–Joyner–Halenda method, respectively. According to N_2-BET measurements, the average pore diameters, surface areas, and pore volumes are 6.72 nm, 93.59 $m^2\ g^{-1}$, and 0.571 $cm^3\ g^{-1}$ for MWCNTs, and 13.4 nm, 131.3 $m^2\ g^{-1}$, and 0.427 $cm^3\ g^{-1}$ for MWCNT-*g*-pMMA, respectively.

TGA–DTA measurements were performed by using a Shimadzu TGA-50 thermogravimetric analyzer from 25 to 800 °C at the heating rate of 10 °C min^{-1} with an air flow rate of 50 mL min^{-1}. The samples of 4,4′-DCB adsorbed MWCNTs and MWCNT-*g*-pMMA were prepared in 60 mL serum bottles (sealed with rubber septa and aluminum seals) at $T = 20 \pm 1$ °C, initial concentration of 4,4′-DCB 4.14×10^{-3} g L^{-1}, $m/V = 0.03$ g L^{-1}, $C[NaClO_4] = 0.01$ M, and pH = 3.55 ± 0.02. After the adsorption equilibrium, the suspensions were repeatedly rinsed with Milli-Q water until no 4,4′-DCB in the supernatant was detected by using GC-ECD method. At last, the samples were dried in oven at 95 °C for 24 h, and thus 4,4′-DCB adsorbed MWCNTs and 4,4′-DCB adsorbed MWCNT-*g*-pMMA samples were obtained.

2.4. Adsorption of 4,4′-DCB on MWCNTs and MWCNT-g-pMMA

The adsorption of 4,4′-DCB on MWCNT-*g*-pMMA and MWCNTs were carried out at $T = 20 \pm 1$ °C in 60 mL serum bottles, sealed with rubber septa and aluminum seals. The stock suspension of adsorbents, $NaClO_4$, $HClO_4$ and 4,4′-DCB (containing 1.0% (V/V) of methanol) solution were added to achieve the desired concentrations

of different components. The pH values of the suspensions were adjusted to 3.55 ± 0.05 by adding negligible volumes of 0.1 or 0.01 M $HClO_4$ and/or NaOH. After the suspensions were shaken for 50 h, the solid and liquid phases were separated by centrifugation at 3000 rpm for 30 min, and then the supernatant was filtered using 0.45 μm membrane filter. The concentration of 4,4′-DCB in supernatant was analyzed by gas chromatography equipped with electron capture detector (GC-ECD). The GC-ECD analysis was performed on a Hewlett–Packard 5890 chromatograph equipped with a DB-5 column (50 m × 0.32 mm × 0.17 mm) using high purity nitrogen as carrier gas.

The adsorption percentage of 4,4′-DCB on MWCNTs and MWCNT-*g*-pMMA was calculated from the difference between the initial concentration (C_0) of 4,4′-DCB in suspension and the final one (C_{eq}) of 4,4′-DCB in supernatant after centrifugation:

$$\text{Adsorption}\% = \frac{C_0 - C_{eq}}{C_0} \times 100\% \quad (1)$$

The amount of 4,4′-DCB adsorbed on the solid phase (C_s) was calculated from the initial concentration (C_0), the final one (C_{eq}), the volume of the suspension (V), and the mass of the adsorbent ($m_{adsorbent}$):

$$C_s = \frac{C_0 - C_{eq}}{m_{adsorbent}} \times V \quad (2)$$

3. Results and discussion

3.1. Characterization of MWCNTs and MWCNT-g-pMMA

The microstructure transformations of MWCNTs and MWCNT-*g*-pMMA are observed by SEM. MWCNT-*g*-pMMA (Fig. 1B) have a more compact stacking morphology as compared to MWCNTs (Fig. 1A). This is due to the strong interaction between the oxygen-containing functional groups of MMA on the external sidewalls of MWCNTs. The polystyrene and diamine modified MWCNTs by chemical methods also showed very similar SEM images to MWCNT-*g*-pMMA (Fan et al., 2007; Meng et al., 2008). Moreover, owing to the grafted MMA on the surfaces of MWCNT-*g*-pMMA, the diameter of MWCNT-*g*-pMMA (20–40 nm) is larger than that of MWCNTs (20–30 nm).

The Raman spectra of MWCNTs and MWCNT-*g*-pMMA are shown in Fig. 1C. The peak at 1352 cm^{-1} is attributed to the disordered structure of MWCNTs (D mode, first-order), such as the defects in the curved graphite sheet, sp^3 carbon, or other impurities. The peak at 1580 cm^{-1} is attributed to the graphite structure of MWCNTs (G mode, first-order), which corresponds to the movement of two neighboring carbon atoms in a graphitic sheet in opposite direction. The peak at 2706 cm^{-1} is for the graphite structure of MWCNTs (G′ mode, second-order) (Zhou et al., 2005; Antunes et al., 2006; Hong et al., 2006; Yi et al., 2006). The values of I_D/I_G ratio are 0.72 for MWCNTs and 1.00 for MWCNT-*g*-pMMA, which reveals that the disorder degree of MWCNT-*g*-pMMA surfaces increases after MWCNTs are grafted with MMA molecules.

XPS is an effective technique for the surface analysis, which is sensitive to identify functional groups attached to MWCNT surfaces. The high resolution XPS C 1s spectra of MWCNTs and MWCNT-*g*-pMMA are shown in Fig. 1D. The C 1s spectra of MWCNTs and MWCNT-*g*-pMMA are deconvoluted into five components: (1) the peak at 284.0 ± 0.2 eV is attributed to the sp^2-hybridized graphite-like carbon atoms (C═C); (2) the peak at 285.0 ± 0.2 eV is due to the sp^3-hybridized carbon (C—C); and (3) the peaks at 286.2 ± 0.2, 287.2 ± 0.2 and 289.0 ± 0.2 eV are considered to originate in carbon atoms bound to one, two, and three oxygen atoms, respectively. Because electronegative oxygen atoms induce a positive charge on carbon atoms (Ago et al., 1999; Liu et al., 2008), they correspond to C—O (e.g., alcohol, ether), C═O (e.g., ketone, aldehyde) and O—C═O (e.g., carboxylic, ester) species, respectively. The results of the XPS analysis (Fig. 1D and Table 1) indicate that the relative contents of C═C, C—O, O—C═O on MWCNTs decrease, whereas the C—C and C═O components on MWCNT-*g*-pMMA increase after plasma induced grafting with MMA. The XPS analysis indicate that MMA molecules are grafted on the hydroxyl sites of MWCNTs (corresponding to the decreasing of the peak components of C—O and O—C═O) or grafted on the framework of MWCNTs (corresponding to the decreasing of C═C components), which improves the disorder degree of MWCNT-*g*-pMMA surfaces.

The thermal properties of MWCNTs and MWCNT-*g*-pMMA are evaluated by TGA–DTA analysis (Fig. 1E). According to the TGA–DTA curves of MWCNTs, the carbon impurity (such as amorphous carbon) in MWCNTs is negligible, and MWCNTs decompose at 477.6–682.7 °C (endothermic). Compared to MWCNTs, MWCNT-*g*-pMMA are less thermal stable responding for the grafted MMA on MWCNT surfaces. The TGA–DTA curves of MWCNT-*g*-pMMA show the characteristic peaks of MMA. The mass loss of 0.78% at 24.7–128.8 °C is due to the loss of the absorbed water. The mass loss of 8.06% at 151.2–461.0 °C (exothermic) corresponds to the decomposition of MMA (Uyar et al., 2005, 2006). The mass loss of 89.9% at 469.5–665.4 °C (exothermic) corresponds to the combustion of MWCNTs. From the TGA–DTA analysis, the mass percentage of grafted MMA on MWCNT-*g*-pMMA is ~8.1%.

Fig. 1F presents the XRD patterns of MWCNTs and MWCNT-*g*-pMMA. The peaks at 2θ = 10.3, 26.2, 43.0, and 53.7° are related to the characteristics of MWCNTs. The XRD patterns of MWCNTs and MWCNT-*g*-pMMA are very similar, indicating that little alteration in the structure of MWCNTs occurs in the MMA grafting process. The plasma induced grafting process only occurs on MWCNT surfaces and does not destroy the framework of MWCNTs.

Fig. 1G shows the acid–base titration curves of MWCNTs and MWCNT-*g*-pMMA. The acid–base titrations of MWCNTs and MWCNT-*g*-pMMA were consumed by the following steps: neutralization of excess H^+ in suspensions firstly, then reacted with the various receivers on adsorbent surfaces, and at last adjustment of the suspension pH. In order to calculate the concentration of acid and basic sites of MWCNTs and MWCNT-*g*-pMMA, constant capacity model and non-linear optimization program FITEQL 3.1 were applied to simulate the potentiometric titration data. A heterogeneous surface reaction scheme, which assumed a surface consisting of non-equivalent classes of amphoteric binding sites, was used to model titration data. The acid–base equilibriums on the surfaces of MWCNTs and MWCNT-*g*-pMMA were represented by the following reactions:

$$-\text{XOH} + \text{H}^+ \iff -\text{XOH}_2^+ \quad \text{K}_{\text{X}-1}^{\text{int}} = \frac{[-\text{XOH}_2^+]}{[-\text{XOH}] \times [\text{H}_s^+]} \quad (3)$$

$$-\text{XOH} \iff -\text{XO}^- + \text{H}_s^+ \quad \text{K}_{\text{X}-2}^{\text{int}} = \frac{[-\text{XO}^-] \times [\text{H}_s^+]}{-[\text{XOH}]} \quad (4)$$

where $-XOH_2^+$, $-XOH$, and $-XO^-$ represent positively charged, neutral, and negatively charged sites on MWCNTs and MWCNT-*g*-pMMA, respectively. H_s^+ is the proton concentration on sample surfaces.

According to the simulation results, K_{X-1}^{int}, K_{X-2}^{int}, and total concentration of surface sites are 3.10, 4.98, and 1.12×10^{-4} mol g^{-1} for MWCNTs; and 4.30, 5.24, and 6.79×10^{-4} mol g^{-1} for MWCNT-*g*-pMMA, respectively. The total concentration of surface sites on MWCNT-*g*-pMMA is much higher than that on MWCNTs. The high concentration of surface sites is attributed to the functional groups of grafted MMA on MWCNT-*g*-pMMA. Moreover,

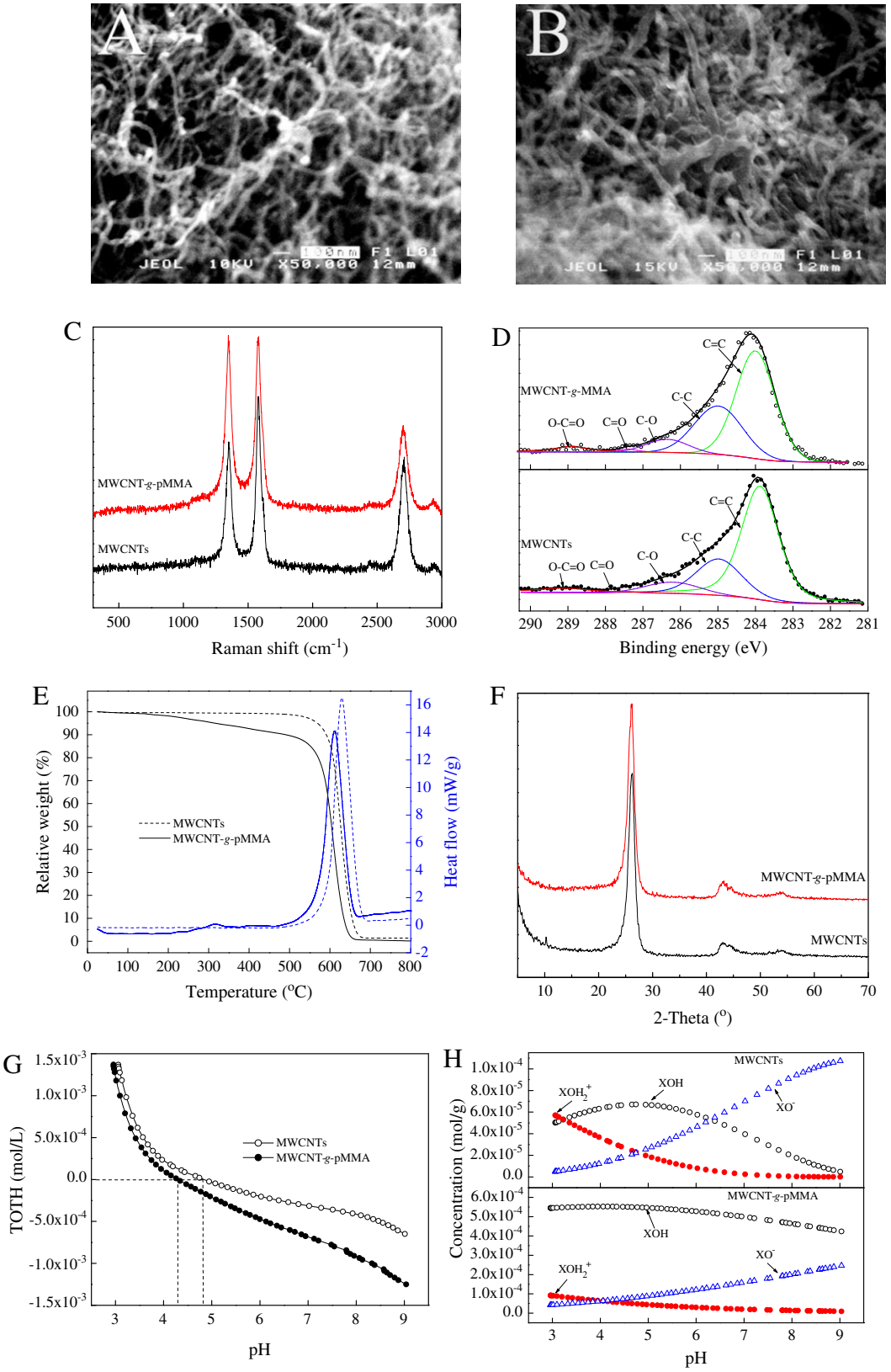

Fig. 1. Characterization of MWCNTs and MWCNT-*g*-pMMA. SEM images of MWCNTs (A) and MWCNT-*g*-pMMA (B); Raman spectra (C); XPS C 1s spectra (D); TGA–DTA curves (E); XRD patterns (F); total concentration of consumed protons (TOTH) curves (m/V = 5.0 g L^{-1}) (G); and site concentration distribution as a function of pH (H).

Table 1
Curve fitting results of XPS C 1s spectra.

	C═C (%)	C—C (%)	C—O (%)	C═O (%)	O—C═O (%)
MWCNTs	63.9	23.3	7.76	0.32	4.70
MWCNT-*g*-pMMA	55.1	32.6	7.69	1.18	3.52

the distribution of the species is influenced by pH values significantly (Fig. 1H). The concentration of $-XOH_2^+$ species decreases with increasing pH, whereas the concentration of $-XO^-$ species increases with increasing pH values.

According to the characterization results and the optical emission spectroscopy of N_2 plasma (Fig. 2A), the mechanism of N_2 plasma induced grafting MMA on MWCNTs is proposed in Fig. 2B. The active nitrogen species (N^*) are generated under the N_2 plasma conditions, and then react with MWCNTs to form active species ($—C^*$) on the frameworks of MWCNTs (which reduces C═C component) or at the defect sites of MWCNTs (which reduces C—O and O—C═O components) in N_2 plasma discharging process. After MMA solution is added to the grafting reactor, the $—C^*$ species can react with MMA molecules. The binding energy of C═C is lower than that of other groups in MMA molecule, and the $—C^*$ species can react with MMA molecule at the C═C sites of MMA likely. The C═C sites of MMA carries active species after the reaction with the $—C^*$ active species on MWCNT surfaces, which can also react with other MMA molecules and induces the polymerization of MMA on MWCNT surfaces. Thus MMA molecules are grafted on the surfaces of MWCNTs by surface initiated radical polymerization.

3.2. Adsorption of 4,4′-DCB on MWCNTs and MWCNT-g-pMMA

In order to evaluate the application of MWCNT-*g*-pMMA in real work, the adsorption of 4,4′-DCB from aqueous solution on MWCNTs and MWCNT-*g*-pMMA were studied. More than 95% removal of 4,4′-DCB was removed from aqueous solution to MWCNTs or MWCNT-*g*-pMMA in the first 24 h of contact time, and less than 5% additional removal of 4,4′-DCB was achieved in the following 24 h of contact time (Fig. 3). Nollet et al. (2003) reported that the adsorption of 2,3,4-trichlorobiphenyl (2,3,4-TCB) and 2,2′,3,3′,4,5,6-heptachlorobiphenyl (2,2′,3,3′,4,5,6-HeCB) on the fly ash reached equilibrium after the contact time of 50 h. Moreover, ~90–97% removal of 2,3,4-TCB and 2,2′,3,3′,4,5,6-HeCB occurred in the first 24 h of contact time depending on the initial concentrations, and only ~2–5% additional removal was achieved

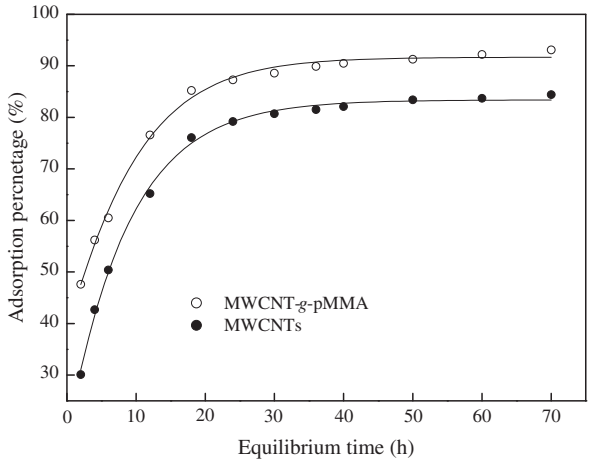

Fig. 3. Effect of contact time on the removal of 4,4′-DCB from solution to MWCNT-*g*-pMMA and MWCNTs. $T = 20 \pm 1$ °C, $C[4,4'\text{-DCB}]_{initial} = 4.14 \times 10^{-3}$ g L^{-1}, $m/V = 0.03$ g L^{-1}, pH = 3.55 ± 0.02, $C[NaClO_4] = 0.01$ M.

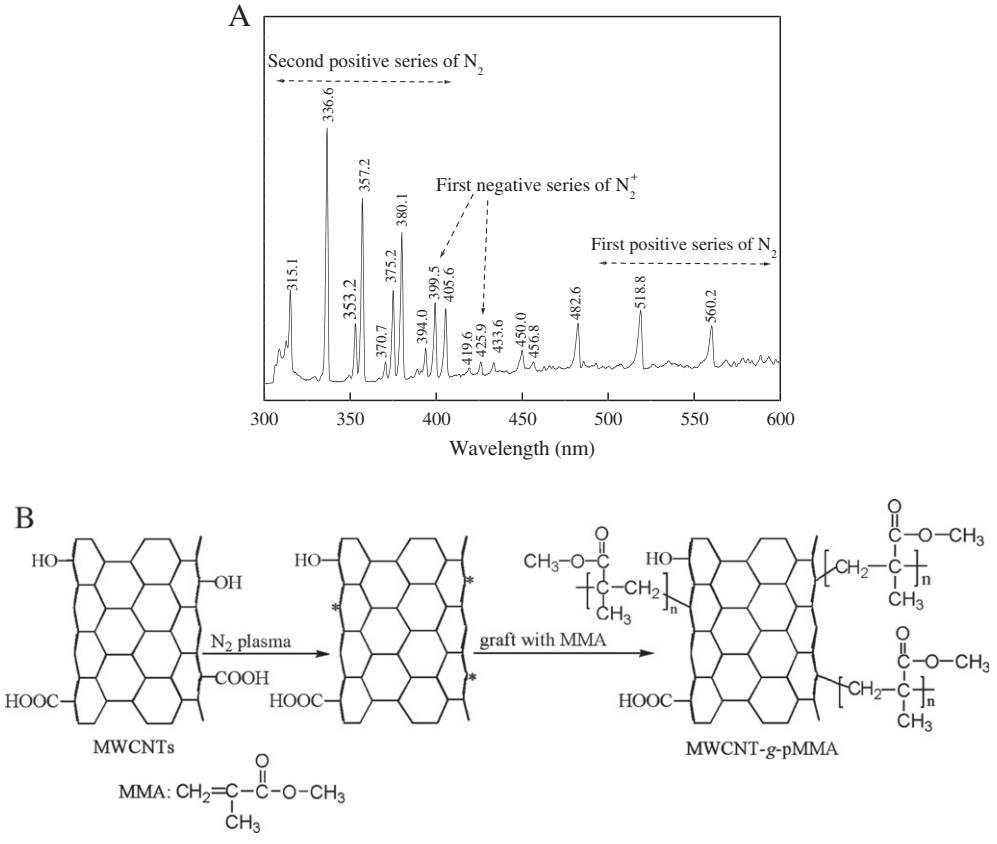

Fig. 2. The optical emission spectroscopy of N_2 plasma (A) and proposed mechanism of grafting MMA on MWCNTs (B).

in the following 24 h of contact time. Yang et al. (2007) reported that the adsorption of 2,4,5-trichlorobiphenyl (2,4,5-TCB) and biphenyl on the activated carbon felt (ACF) reached equilibrium in 20 min. From the kinetic adsorption experiments, the adsorption of 4,4′-DCB on MWCNT-*g*-pMMA was selected to 50 h in the experiments.

In the removal of PCBs from aqueous solutions, the amount of adsorbent is crucial for the economic application. Under the effective removal percentage uncertainties, the less amount of adsorbent is used, the lower cost is applied. The effect of adsorbent content on the adsorption of 4,4′-DCB is shown in Fig. 4A. The strong adsorption of 4,4′-DCB on MWCNTs is mainly attributed to the electron donor–acceptor interaction of 4,4′-DCB on the graphene surface of MWCNTs, and also the hydrogen bonds between hydrogen of the benzene ring of 4,4′-DCB with the oxygen-containing functional groups on MWCNT surfaces (Long and Yang, 2001; Pan and Xing, 2008). The interaction between 2,4,5-TCB (or biphenyl) and ACF was irreversible chemical adsorption, and the desorption of 2,4,5-TCB (or biphenyl) from ACF was difficult (Yang et al., 2007) because the p-systems of PCB rings can behave as electron donor (Sotelo et al., 2002). Therefore, 4,4′-DCB with the grapheme surface of MWCNTs can form electron donor–acceptor interactions.

The adsorption percentage of 4,4′-DCB on MWCNT-*g*-pMMA is markedly higher than that of 4,4′-DCB on MWCNTs at the same solid content. One can see that more than 90% 4,4′-DCB is adsorbed on MWCNT-*g*-pMMA even if the solid content is only 0.03 g L^{-1}, which indicates that MWCNT-*g*-pMMA have very high adsorption ability in the removal of 4,4′-DCB from large volumes of aqueous solutions. From the acid–base titration results, the surface site concentration on MWCNT-*g*-pMMA is much high than that on MWCNTs. The XPS analysis also indicates that the grafted pMMA can provide more functional groups to form complexes with 4,4′-DCB. The carboxylic groups of pMMA can form electron donor–acceptor complexes with 4,4′-DCB on MWCNT-*g*-pMMA surfaces (Peng et al., 2003; Shieh and Liu, 2003). The electron donor aromatic rings of 4,4′-DCB and the electron acceptor of the graphene surface of MWCNTs can also form electron donor–acceptor interactions (Sotelo et al., 2002; Pan and Xing, 2008). The hydrogen of the benzene ring of 4,4′-DCB can also form hydrogen bonds with the carboxylic groups of pMMA, and thereby increases the adsorption of 4,4′-DCB on MWCNT-*g*-pMMA (Yampolskii and Bondarenko, 1998; Roth and Torkelson, 2007). The grafted MMA on MWCNT-*g*-pMMA improves the adsorption ability of MWCNT-*g*-pMMA obviously.

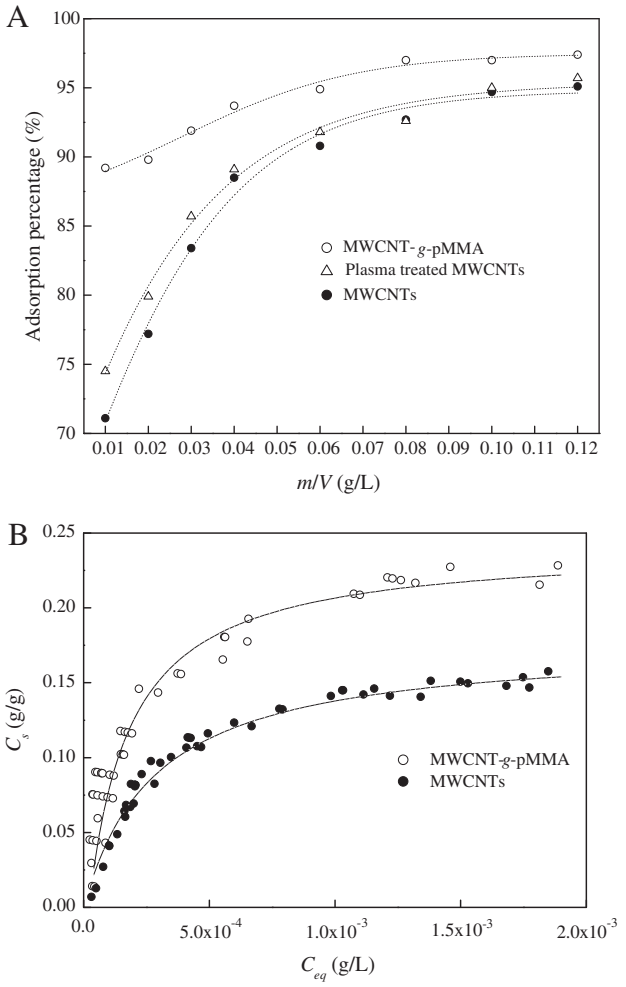

Fig. 4. Effect of solid content on 4,4′-DCB adsorption to MWCNTs, plasma treated MWCNTs and MWCNT-*g*-pMMA (A) and adsorption isotherms (B). $T = 20 \pm 1$ °C, equilibrium time 50 h, pH = 3.55 ± 0.02, C[$NaClO_4$] = 0.01 M. (A): $C[4,4'\text{-DCB}]_{initial} = 4.14 \times 10^{-3}$ g L^{-1}; (B): $m/V = 0.03$ g L^{-1}.

Fig. 4A also shows that the adsorption curve of 4,4′-DCB on plasma treated MWCNTs is a little higher than that of 4,4′-DCB on MWCNTs. It is reasonable because the surfaces of MWCNTs become rough, and the surface defects are enhanced after the N_2 plasma treatment process.

The adsorption isotherms of 4,4′-DCB on MWCNT-*g*-pMMA and MWCNTs are shown in Fig. 4B. The experimental data are well simulated by Langmuir model ($C_s = \frac{bC_{smax}C_{eq}}{1+bC_{eq}}$, C_{smax} is the maximum adsorption capacity, and b is Langmuir constant). The b and C_{smax} values calculated from Langmuir model are ~6.0 and ~0.240 g g^{-1} for 4,4′-DCB on MWCNT-*g*-pMMA, and ~3.5 and ~0.177 g g^{-1} for 4,4′-DCB on MWCNTs under the experimental conditions, respectively.

Effect of pH on 4,4′-DCB adsorption to MWCNT-*g*-pMMA is shown in Fig. 5A. The removal of 4,4′-DCB on MWCNT-*g*-pMMA fluctuates very little in pH ranging from 2 to 10, which suggests that MWCNT-*g*-pMMA are excellent adsorbents for 4,4′-DCB removal from large volumes of aqueous solutions. When pH exceeds 10, the adsorption of 4,4′-DCB on MWCNT-*g*-pMMA decreases with increasing pH values. This can be due to the fact that more oxygen containing groups (such as —COOH and —OH) on MWCNT-*g*-pMMA surfaces are ionized (carrying negative charge) at high pH values and thus adsorb more water molecules. The formation of water cluster on oxygen containing groups blocks the access of 4,4′-DCB to the adsorption sites of MWCNT-*g*-pMMA and thereby results in less adsorption of 4,4′-DCB (Peng et al., 2003; Lu et al., 2005). Nollet et al. (2003) reported that no significant differences were found for the adsorption of 2,3,4-TCB and 2,2′,3,3′,4,5,6-HeCB on the fly ash at different pH values. Lu et al. (2005) reported that the adsorption of trihalomethanes on MWCNTs fluctuated very little in pH ranging from 3 to 7, and decreased with increasing pH at pH > 7. The pH-independent adsorption of 4,4′-DCB on MWCNT-*g*-pMMA at pH < 10 is quite important for the application of MWCNT-*g*-pMMA in PCB pollution cleanup in real work.

Fig. 5B shows that the adsorption of 4,4′-DCB on MWCNT-*g*-pMMA is independent of $NaClO_4$ concentrations. 4,4′-DCB is non-ionic chemical and the properties of 4,4′-DCB is not affected by pH and ionic strength of aqueous solutions. The results are very interesting and important for the application of MWCNT-*g*-pMMA in the removal of organic pollutants from wastewater. In wastewater, the salt concentration may be different. The ionic strength-independent adsorption of 4,4′-DCB on MWCNT-*g*-pMMA is crucial for the evaluation of MWCNT-*g*-pMMA in wastewater cleanup management. In the PCB pollution cleanup, it is not necessary to consider different salt concentrations and pH values at different areas in real work.

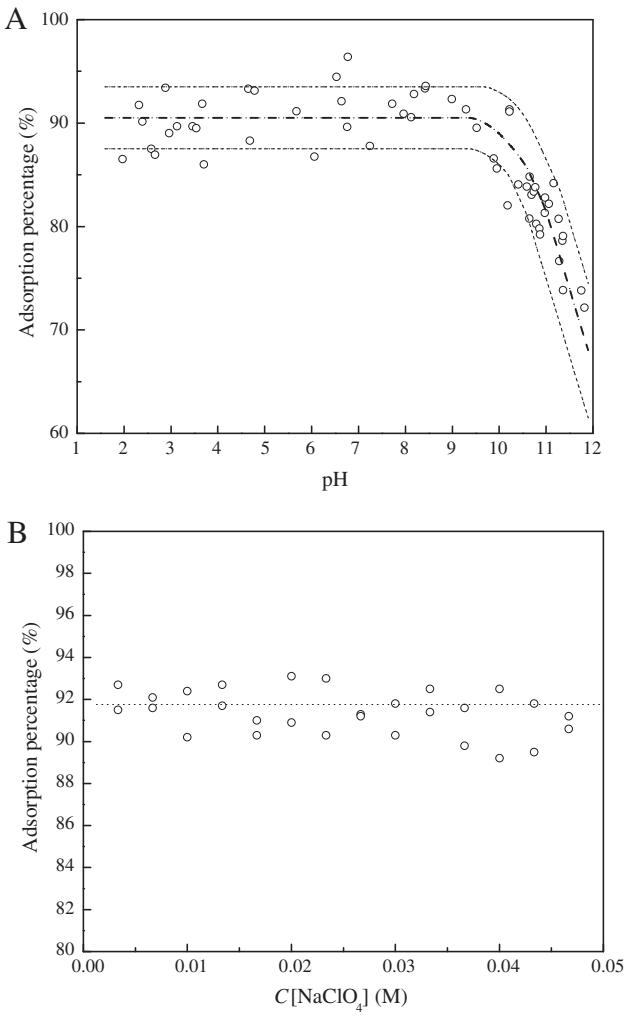

Fig. 5. Effect of pH (A) and ionic strength (B) on the removal of 4,4′-DCB from solution to MWCNT-*g*-pMMA. $T = 20 \pm 1$ °C, equilibrium time 50 h, $C[4,4'\text{-DCB}]_{initial} = 4.14 \times 10^{-3}$ g L^{-1}, $m/V = 0.03$ g L^{-1}. (A): $C[NaClO_4] = 0.01$ M; (B): pH = 3.55 ± 0.02.

3.3. Thermal regeneration

In order to study the thermal desorption of 4,4′-DCB from MWCNT-*g*-pMMA, the TGA–DTA curves of MWCNTs and MWCNT-*g*-pMMA before and after the adsorption of 4,4′-DCB were carried out. As can be seen from the TGA–DTA curves of MWCNTs and MWCNT-*g*-pMMA before and after the adsorption of 4,4′-DCB (Fig. 6), the adsorbed 4,4′-DCB on MWCNTs was thermally decomposed step by step in the temperature programming processes. The thermal decomposition of 4,4′-DCB from MWCNT-*g*-pMMA was difficult as compared to that of 4,4′-DCB from MWCNTs. Moreover, the adsorbed 4,4′-DCB on MWCNT-*g*-pMMA can restrain the decomposition of MWCNT-*g*-pMMA for the strong interaction of 4,4′-DCB with MWCNT-*g*-pMMA.

The desorption temperature of organic compounds from adsorbents is related to its bond strength with adsorbents, and stronger bond are related to a higher desorption temperature (Long and Yang, 2001). In our previous study, we found that the desorption of 4,4′-DCB adsorbed on β-cyclodextrin modified MWCNTs is very difficult because the modified β-cyclodextrin on MWCNT surfaces can form strong inclusion complexes with 4,4′-DCB (Shao et al., 2010). The thermal decomposition of 4,4′-DCB from MWCNT-*g*-pMMA was difficult as compared to that of 4,4′-DCB from

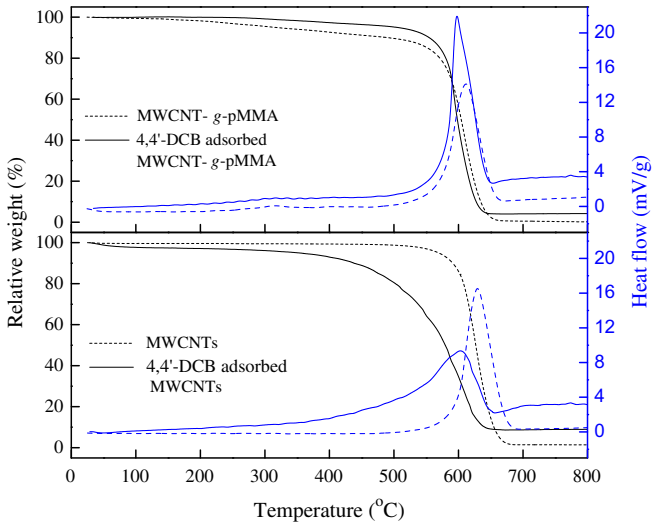

Fig. 6. TGA–DTA curves of MWCNTs and MWCNT-*g*-pMMA before and after the adsorption of 4,4′-DCB.

MWCNTs, which is due to the strong interaction between 4,4′-DCB and pMMA on MWCNT surfaces. The result is very interesting because the potential pollution of 4,4′-DCB caused by the desorption and thermal decomposition of 4,4′-DCB from MWCNT-*g*-pMMA can be negligible. From the results of adsorption and TGA–DTA analysis, one can draw the conclusion that MWCNT-*g*-pMMA are very suitable materials for the preconcentration and solidification of PCBs from large volumes of aqueous solutions in PCB pollution cleanup.

4. Conclusions

MMA molecules are grafted on MWCNT surfaces by using a N_2 plasma technique. The SEM images suggest that the smooth surfaces of MWCNTs become rough and their average diameter becomes larger after plasma grafting treatment. Raman analysis indicates that the disorder degree of MWCNT-*g*-pMMA increases. XPS analysis shows that the plasma technique is a very efficient method to graft MMA on MWCNTs. Acid–base tradition analysis indicates that the surface site concentration of MWCNT-*g*-pMMA is much higher than that of MWCNTs. MWCNT-*g*-pMMA have very high adsorption ability in the removal of 4,4′-DCB from large volumes of aqueous solutions. The adsorption of 4,4′-DCB on MWCNT-*g*-pMMA is independent of ionic strength and pH values over a large range. MWCNT-*g*-pMMA are very suitable materials for the preconcentration and immobilization of PCBs in PCB pollution cleanup.

Acknowledgements

Financial support from National Natural Science Foundation of China (21007074; 21077107; 20971126; 20907055), 973 Projects from Ministry of Science and Technology (2007CB936602; 2011CB933700), and the Open Fund of State Key Laboratory of Estuarine and Coastal Research are acknowledged.

References

Adeel, Z., Luthy, R.G., Dzombak, D.A., Roy, S.B., Smith, J.R., 1997. Leaching of PCB compounds from untreated and biotreated sludge-soil mixtures. J. Contam. Hydrol. 28, 289–309.

Ago, H., Kugler, T., Cacialli, F., Salaneck, W.R., Shaffer, M.S.P., Windle, A.H., Friend, R.H., 1999. Work functions and surface functional groups of multiwall carbon nanotubes. J. Phys. Chem. B 103, 8116–8121.

Antunes, E.F., Lobo, A.O., Corat, E.J., Trava-Airoldi, V.J., Martin, A.A., Veríssimo, C., 2006. Comparative study of first- and second- order Raman spectra of MWCNT at visible and infrared laser excitation. Carbon 44, 2202–2211.

Baskaran, D., Mays, J.W., Bratcher, M.S., 2004. Polymer-grafted multiwalled carbon nanotubes through surface-initiated polymerisation. Angew. Chem. Int. Ed. 43, 2138–2142.

Chevallier, P., Castonguay, M., Turgeon, S., Dubrulle, N., Mantovani, D., McBreen, P.H., Wittmann, J.C., Laroche, G., 2001. Ammonia RF plasma on PTFE surfaces: chemical characterization of the species created on the surface by vapor phase chemical derivatization. J. Phys. Chem. B 105, 12490–12497.

Das, S., Banthia, A.K., Adhikari, B., 2006. Removal of chlorinated volatile organic contaminants from water by pervaporation using a novel polyurethane urea–poly (methyl methacrylate) interpenetrating network membrane. Chem. Eng. Sci. 61, 6454–6467.

Dubreuil, A.C., Doumenc, F., Guerrier, B., Johannsmann, D., Allain, C., 2003. Analysis of the solvent diffusion in glassy polymer films using a set inversion method. Polymer 44, 377–387.

Endo, S., Takizawa, R., Okuda, K., Takada, H., Chiba, K., Kanehiro, H., Ogi, H., Yamashita, R., Date, T., 2005. Concentration of polychlorinated biphenyls (PCBs) in beached resin pellets: variability among individual particles and regional differences. Mar. Pollut. Bull. 50, 1103–1114.

Fan, D., He, J., Tang, W., Xu, J., Yang, Y., 2007. Synthesis of polymer grafted carbon nanotubes by nitroxide mediated radical polymerization in the presence of spin-labeled carbon nanotubes. Eur. Polym. J. 43, 26–34.

Gjessing, E.T., Steiro, C., Becher, G., Christy, A., 2007. Reduced analytical availability of polychlorinated biphenyls (PCB's) in colored surface water. Chemosphere 66, 644–649.

Gotovac, S., Hattori, Y., Noguchi, D., Miyamoto, J., Kanamaru, M., Utsumi, S., Kanoh, H., Kanako, K., 2006. Phenanthrene adsorption from solution on single wall carbon nanotubes. J. Phys. Chem. B 110, 16219–16224.

Hong, C., You, Y., Pan, C., 2006. A new approach to functionalize multi-walled carbon nanotubes by the use of functional polymers. Polymer 47, 4300–4309.

Hwang, G.L., Shieh, Y.T., Hwang, K.C., 2004. Efficient load transfer to polymer-grafted multiwalled carbon nanotubes in polymer composites. Adv. Funct. Mater. 14, 487–491.

Iijima, S., 1991. Helical microtubules of graphic carbon. Nature 354, 56–58.

Kong, H., Gao, C., Yan, D., 2004. Controlled functionalization of multiwalled carbon nanotubes by in situ atom transfer radical polymerization. J. Am. Chem. Soc. 126, 412–413.

Koshio, A., Yudasaka, M., Zhang, M., Iijima, S., 2001. A simple way to chemically react single-wall carbon nanotubes with organic materials using ultrasonication. Nano Lett. 1, 361–363.

Lewis, G.T., Nowling, G.R., Hicks, R.F., Cohen, Y., 2007. Inorganic surface nanostructuring by atmospheric pressure plasma-induced graft polymerization. Langmuir 23, 10756–10764.

Li, H., Xu, M., Shi, Z., He, B., 2004. Isotherm analysis of phenol adsorption on polymeric adsorbents from nonaqueous solution. J. Colloid Interface Sci. 271, 47–54.

Liu, G.H., Wang, J.L., Zhu, Y.F., Zhang, X.R., 2004. Application of multiwalled carbon nanotubes as a solid-phase extraction sorbent for chlorobenzenes. Anal. Lett. 37, 3085–3104.

Liu, Y., Yu, Z., Zhang, Y., Guo, D., Liu, Y., 2008. Supramolecular architectures of β-cyclodextrin-modified chitosan and pyrene derivatives mediated by carbon nanotubes and their DNA condensation. J. Am. Chem. Soc. 130, 10431–10439.

Long, Q.R., Yang, R.T., 2001. Carbon nanotubes as superior sorbent for dioxin removal. J. Am. Chem. Soc. 123, 2058–2059.

Lu, C., Chung, Y.L., Chang, K.F., 2005. Adsorption of trihalomethanes from water with carbon nanotubes. Water Res. 39, 1183–1189.

Meng, H., Sui, G., Fang, P., Yang, R., 2008. Effects of acid- and diamine-modified MWNTs on the mechanical properties and crystallization behavior of polyamide 6. Polymer 49, 610–620.

Nollet, H., Roels, M., Lutgen, P., Meeren, P., Verstraete, W., 2003. Removal of PCBs from wastewater using fly ash. Chemosphere 53, 655–665.

Olander, B., Wirsén, A., Albertsson, A.C., 2002. Argon microwave plasma treatment and subsequent hydrosilylation grafting as a way to obtain silicone biomaterials with well-defined surface structures. Biomacromolecules 3, 505–510.

Pan, B., Xing, B., 2008. Adsorption mechanisms of organic chemicals on carbon nanotubes. Environ. Sci. Technol. 42, 9005–9013.

Pascall, M.A., Zabik, M.E., Zabik, M.J., Hernandez, R.J., 2005. Uptake of polychlorinated biphenyls (PCBs) from an aqueous medium by polyethylene, polyvinyl chloride, and polystyrene films. J. Agric. Food Chem. 53, 164–169.

Peng, X., Li, Y., Luan, Z., Di, Z., Wang, H., Tian, B., Tian, B., Jia, Z., 2003. Adsorption of 1, 2-dichlorobenzene from water to carbon nanotubes. Chem. Phys. Lett. 376, 154–158.

Pyrzynska, K., Stafiej, A., Biesaga, M., 2007. Sorption behavior of acidic herbicides on carbon nanotubes. Microchim. Acta 159, 293–298.

Qin, S., Qin, D., Ford, W.T., Resasco, D.E., Herrera, J.E., 2004. Polymer brushes on single-walled carbon nanotubes by atom transfer radical polymerization of n-butyl methacrylate. J. Am. Chem. Soc. 126, 170–176.

Roth, C.B., Torkelson, J.M., 2007. Selectively probing the glass transition temperature in multilayer polymer films, equivalence of block copolymers and multilayer films of different homopolymers. Macromolecules 40, 3328–3336.

Shao, D., Jiang, Z., Wang, X., Li, J., Meng, Y., 2009. Plasma induced grafting carboxymethyl cellulose on multiwalled carbon nanotubes for the removal of UO_2^{2+} from aqueous solution. J. Phys. Chem. B 113, 860–864.

Shao, D., Sheng, G., Chen, C., Wang, X., Nagatsu, M., 2010. Removal of polychlorinated biphenyls from aqueous solutions using β-cyclodextrin grafted multiwalled carbon nanotubes. Chemosphere 79, 679–685.

Shen, J., Zheng, X., Ruan, H., Wu, L., Qiu, J., Gao, C., 2007. Synthesis of AgCl/PMMA hybrid membranes and their sorption performance of cyclohexane/cyclohexene. J. Membr. Sci. 304, 118–124.

Shieh, Y.T., Liu, K.H., 2003. The effect of carbonyl group on sorption of CO_2 in glassy polymers. J. Supercrit. Fluids 25, 261–268.

Skoglund, R.S., Stange, K., Swackhamer, D.L., 1996. A kinetics model for predicting the accumulation of PCBs in phytoplankton. Environ. Sci. Technol. 30, 2113–2120.

Sober, A., Cornelissen, G., Tiselius, P., Gustafsson, Ö., 2006. Passive partitioning of polychlorinated biphenyls between seawater and zooplankton, a study comparing observed field distributions to equilibrium sorption experiments. Environ. Sci. Technol. 40, 6703–6708.

Sotelo, J.L., Ovejero, G., Delgado, J.A., Martínez, I., 2002. Comparison of adsorption equilibrium and kinetics of four chlorinated organics from water onto GAC. Water Res. 36, 599–608.

Uyar, T., Rusa, C.C., Hunt, M.A., Aslan, E., Hacaloglu, J., Tonelli, A.E., 2005. Reorganization and improvement of bulk polymers by processing with their cyclodextrin inclusion compounds. Polymer 46, 4762–4775.

Uyar, T., Aslan, E., Tonelli, A.E., Hacaloglu, J., 2006. Pyrolysis mass spectrometry analysis of poly(vinyl acetate), poly(methyl methacrylate) and their blend coalesced from inclusion compounds formed with γ-cyclodextrin. Polym. Degrad. Stab. 91, 1–11.

Wang, S.G., Liu, X.W., Gong, W.X., Nie, W., Gao, B.Y., Yue, Q.Y., 2007. Adsorption of fulvic acids from aqueous solutions by carbon nanotubes. J. Chem. Technol. Biotechnol. 82, 698–704.

Werner, D., Ghosh, U., Luthy, R.G., 2006. Modeling polychlorinated biphenyl mass transfer after amendment of contaminated sediment with activated carbon. Environ. Sci. Technol. 40, 4211–4218.

Yampolskii, Y.P., Bondarenko, G.N., 1998. Evidence of hydrogen bonding during sorption of chloromethanes in copolymers of chloroprene with methyl methacrylate and methacrylic acid. Polymer 39, 2241–2245.

Yang, B., Yu, G., Huang, J., 2007. Electrocatalytic Hydrodechlorination of 2, 4, 5-trichlorobiphenyl on a palladium-modified nickel foam cathode. Environ. Sci. Technol. 41, 7503–7508.

Yi, B., Rajagopalan, R., Foley, H.C., Kim, U.J., Liu, X., Eklund, P.C., 2006. Catalytic polymerization and facile grafting of poly(furfuryl alcohol) to single-wall carbon nanotube: preparation of nanocomposite carbon. J. Am. Chem. Soc. 128, 11307–11313.

Yoon, B.O., Koyanagi, S., Asano, T., Hara, M., Higuchi, A., 2003. Removal of endocrine disruptors by selective sorption method using polydimethylsiloxane membranes. J. Membr. Sci. 213, 137–144.

Zhang, C., Wyatt, J., Weinkauf, D.H., 2004. Carbon dioxide sorption in conventional and plasma polymerized methyl methacrylate thin films. Polymer 45, 7665–7671.

Zhou, L., Ohta, K., Kuroda, K., Lei, N., Matsuishi, K., Gao, L., Matsumoto, T., Nakamura, J., 2005. Catalytic functions of Mo/Ni/MgO in the synthesis of thin carbon nanotubes. J. Phys. Chem. B 109, 4439–4447.